Universität des Saarlandes

Fachrichtung 6.1 – Mathematik

Preprint Nr. 177

Fully Automated Segmentation and Morphometrical Analysis of Muscle Fibre Images

Yoo-Jin Kim, Thomas Brox,
Wolfgang Feiden and Joachim Weickert

Saarbrücken 2006

Fachrichtung 6.1 – Mathematik
Universität des Saarlandes

Preprint No. 177
submitted: July 8, 2006

Fully Automated Segmentation and Morphometrical Analysis of Muscle Fibre Images

Yoo-Jin Kim
Institute of Neuropathology
Saarland University
School of Medicine, Bld. 90.3
66421 Homburg/Saar
Germany
yoo.jin.kim@uniklinik-saarland.de

Thomas Brox
Computer Vision and Pattern Recognition Group
University of Bonn
Römerstraße 164
53117 Bonn
Germany
brox@cs.uni-bonn.de

Wolfgang Feiden
Institute of Neuropathology
Saarland University
School of Medicine, Bld. 90.3
66421 Homburg/Saar
Germany
pawfei@uniklinik-saarland.de

Joachim Weickert
Mathematical Image Analysis Group
Saarland University, Bld. E1 1
P.O. Box 15 11 50
66041 Saarbrücken
Germany
weickert@mia.uni-saarland.de

Edited by
FR 6.1 – Mathematik
Universität des Saarlandes
Postfach 15 11 50
66041 Saarbrücken
Germany

Fax: + 49 681 302 4443
e-Mail: preprint@math.uni-sb.de
WWW: http://www.math.uni-sb.de/

Fully automated segmentation and morphometrical analysis of muscle fibre images

Yoo-Jin Kim[1], Thomas Brox[2], Wolfgang Feiden[1], Joachim Weickert[3]

[1]Institute of Neuropathology, Saarland University, School of Medicine, Homburg/Saar, Germany
[2]Computer Vision and Pattern Recognition Group, University of Bonn, Germany
[3]Mathematical Image Analysis Group, Saarland University, Saarbrücken, Germany

Address for correspondence:
Yoo-Jin Kim, MD
Institute of Neuropathology
Saarland University, School of Medicine
Bldg. 90.3
D-66421 Homburg-Saar
Germany
Phone: +49-6841-1623863
Fax: +49-6841-1623877
E-mail: yoo.jin.kim@uniklinik-saarland.de

Parts of the method described in this paper were presented at the annual meeting of the Reference Centre for Neuromuscular Diseases of the German Society of Neuropathology and Neuroanatomy (DGNN) in Aachen, Germany, April 2005 as well as at the Bildverarbeitung für die Medizin (BVM) 2006 Workshop, Hamburg, Germany, March 2006.

ABSTRACT

Background

Measurement of muscle fibre size and determination of size distribution is important in the assessment of neuromuscular disease. Fibre size estimation by simple inspection is inaccurate and subjective. Manual segmentation and measurement are time-consuming and tedious. We therefore propose an automated image analysis method for objective, reproducible, and time-saving measurement of muscle fibres in routinely hematoxylin-eosin stained cryostat sections.

Methods

The proposed segmentation technique makes use of recent advances in level set based segmentation, where classical edge based active contours are extended by region based cues, such as colour and texture. Segmentation and measurement are performed fully automatically. Multiple morphometric parameters, i.e., cross sectional area, lesser diameter, and perimeter are assessed in a single pass. The performance of the computed method was compared to results obtained by manual measurement by experts.

Results

The correct classification rate of the computed method was high (98%). Segmentation and measurement results obtained manually or automatically did not reveal any significant differences.

Conclusions

The presented region based active contour approach has been proven to accurately segment and measure muscle fibres. Complete automation minimises user interaction, thus, batch processing, as well as objective and reproducible muscle fibre morphometry are provided.

KEY WORDS: automated morphometry – image analysis – segmentation – muscle fibre size

INTRODUCTION

In the assessment of muscular pathology, muscle fibre size and size distribution exhibit basic morphologic as well as diagnostic information. Abnormal deviations, such as atrophy or hypertrophy are difficult to assess subjectively and it is useful to measure morphometrical parameters in hundreds of fibres, in order to compare these with normal data (1,2). It is also important to analyse histological sections quantitatively, since it has been shown that morphometric data can discern very early changes in the distribution pattern of fibre size in muscle biopsy samples (3). The estimation of muscle fibre size by simple inspection - as yet performed in routine diagnostics - is difficult and inaccurate. Practical techniques have included direct measurement using an eye piece micrometer measurement of a projected image or enlarged microphotographs. However, the manual morphometric approach and interpretation of muscle biopsy material is a subjective, tedious, and time-consuming task (4,5). In addition, reliable assessment of morphometric data in muscle biopsy samples is complicated by the necessity of measurements in several different fields within the biopsy in order to avoid selection bias. In view of these impracticable requirements, muscle fibre morphometry may be accomplished most reasonably by automated routines. Automated analysis of muscle fibre images has not yet received much attention and only few segmentation techniques are at hand so far. The reported methods are based on border shape enhancement routines, followed by application of user-defined or histogram-based thresholds, and interactive manual editing. The usability and performance of these semi-automated methods are still limited by inaccurate delineation of fibres as well as the need of special histochemical stains and user interaction (4,6,7). In contrast to these pixel-intensity and -gradient based applications, Klemenčič et al. (8) suggested a semi-automated approach based on active contour models. The practicability of this method is restricted by the need of pointing the approximate centroid of each fibre manually by the investigator. We here propose a method that makes use of recent advances in level set based segmentation, where classical edge based active contours are extended by region based cues, such as the colour and texture of the interior and exterior of the fibre regions. Whereas edge based active contours require an accurate contour initialisation, which is usually provided by manual interaction, as in (8), region based active contours depend less on the initialisation and can therefore ensure a reliable separation process without manual interaction. This leads to an accurate, fully automated methodology that allows for time-saving batch processing of the entire biopsy samples.

MATERIALS AND METHODS

Muscle Sample Preparation

Biopsy samples were trimmed, mounted, and frozen in isopentane-cooled liquid nitrogen, before storage at –70°C. Transverse sections (10 µm) were cut with a cryotome at –20°C and attached to slides by thawing. After keeping the slides at room temperature at least for 30 min., the sections were stained with hematoxylin and eosin.

Image Acquisition

Microscopic images were taken in artefact-free areas in muscle cross sections with a 20x objective (Nikon Eclipse E600 microscope, Nikon DN100 CCD-camera: Nikon, Tokio, Japan) and stored as 640 x 480 pixel (571 x 428 µm) RGB colour images.

Segmentation Method

Combined region and edge based active contour model. The core algorithm for separating the muscle fibres from the connective tissue is based on active contour models as introduced by Kass et al. (9). The method makes use of the level set technique known from (10) and (11). Related level set based active contours are, in particular, edge based geodesic active contours (12,13), and region based active contours, as introduced by Chan and Vese (14), and Paragios and Deriche (15).

In level set based segmentation methods, the sought contour, which separates in this case the two classes of muscle fibres and connective tissue, is represented by the zero-level line of a so-called embedding function ϕ. This implicit representation of the contour has several advantages, among others that parts of the two regions need not necessarily be connected and that they can split and merge. This is essential for the present application, since the region of the muscle fibres itself consists of numerous so-called connected components separated from each other by areas of connective tissue, i.e., it is not connected. For the analysis of the individual fibres it is even required that different fibres result in separated connected components.

Active contour models are variational models, i.e., they are described by a cost functional $E(\phi)$, in which undesirable properties of a possible solution ϕ are penalised by high costs. By minimising the total cost $E(\phi)$, one finds an optimal solution ϕ. In the active contour model used for our method, the energy consists of two parts:

$$E(\phi) = \underbrace{\int_{\Omega} \left(H(\phi) \log p_1 + (1 - H(\phi)) \log p_2 \right) dx}_{\text{Part I}} + \nu \underbrace{\int_{\Omega} g(\nabla I) \left| \nabla H(\phi) \right| dx}_{\text{Part II}} . \quad (1)$$

The first part is region based. Minimizing this part leads to a solution where all pixels within one region are maximally similar with respect to a certain similarity measure. This similarity measure is defined by the region models of the fibres and the tissue given by the probability density functions p_1 and p_2, respectively. The probability density functions are determined from the input image as described further below. The Heaviside function $H(\phi) = 1$ if $\phi > 0$ and $H(\phi) = 0$ if $\phi < 0$ is used to distinguish the two regions given the embedding function ϕ; see (14) for details.

The maximum similarity within regions has the natural consequence that there is additionally a maximum dissimilarity *between* the two regions. This part of the model exploits the fact that the muscle fibres all have a similar colour that can generally be distinguished from the colour of the intermyofibrillar connective tissue.

However, since the colour alone may not always be sufficient to distinguish the two regions, especially because blood vessels can have a very similar colour as the muscle fibres, the colour information is supported by texture information derived by the method described in (16). The muscle fibres are mainly homogeneous without much textural variation, whereas the endomysial connective tissue contains collagenous fibres, blood vessels, fibrocytes, and other cellular components, which are captured by the texture features. Hence, taking also this texture information into account, leads to a more reliable separation of muscle fibres and intermyofibrillar tissue. The texture features used here basically model the magnitude, orientation, and scale of texture elements (16), what makes them similar to Gabor filter responses (17,18). In contrast to Gabor features, however, they have a significantly lower redundancy and encode the texture information in only four channels. The extracted texture features for the sample image in Fig. 2a are shown in Fig. 1.

The three colour channels and the additional four texture channels are combined in the joint probability density functions p_1 and p_2 involved in Equation (1). The channels are assumed to be

independent. Therefore, the probability densities for the fibre and non-fibre regions i=1 and i=2, respectively, can be computed as

$$p_i = \prod_{j=1}^{7} p_{ij} \tag{2}$$

The single channel probability densities p_{ij} are approximated with a Parzen density estimator (19,20,21), which comes down to computing a smoothed histogram in each region i and channel j.

The second part of the energy functional is edge based. Its influence relative to the first part is determined by the weighting parameter ν, which is empirically set to the fixed value $\nu = 2$. From the coloured input image $I = (I_1, I_2, I_3)$ one can compute the inverse gradient magnitude:

$$g(\nabla I) = \frac{1}{\sqrt{\sum_{1}^{3} (\nabla I_k)^2 + 1}} \tag{3}$$

It serves as a weighting function that yields values close to 1 in homogeneous areas of the image and smaller positive values in the presence of edges. The contour that minimizes the second term in (1) is the curve of minimal weighted length. In other words, due to this term, the contour is attracted by edges and prefers to be as short as possible; for details see (12) or (13). This part of the model exploits the fact that the muscle fibres are often separated from the connective tissue by more or less strong edges. It hence supplements a third cue for the partitioning besides the colour and texture information. Moreover, the penalty on the contour length avoids single noise pixels or small artefacts to be separated from the surrounding region.
In order to find the optimum solution according to the energy in (1), one starts with some initial partitioning and then performs a gradient descent that evolves the contour towards solutions with smaller energy. This is achieved by iteratively updating the embedding function, which comprises the contour as its zero-level line. In each iteration, the update is determined by the gradient descent equation derived from the energy functional:

$$\phi^{k+1} = \phi^k + \tau \cdot H'(\phi^k) \cdot \left(\log \frac{p_1(\phi^k)}{p_2(\phi^k)} + \nu \cdot \mathrm{div}\left(g(\nabla I) \frac{\nabla \phi^k}{|\nabla \phi^k|} \right) \right) \tag{4}$$

where k denotes the iteration index and τ the iteration step size. $H'(\phi)$ is the derivative of a smoothed version of the Heaviside function (14). After 200 iterations with $\tau = 0.5$, one obtains the sought contour separating the muscle fibres from the connective tissue; see Figure 1c. Computation times are below 2 minutes on contemporary hardware including texture feature computation.

Setting the initial contour. Due to the region based cues, the active contour model is significantly less sensitive to the initialisation than purely edge based models. Nevertheless, one can slightly improve the segmentation result by setting the initialisation with care. Furthermore, an initialisation that is closer to the sought solution reduces the number of iterations necessary for convergence, and thus, speeds up the algorithm. For these reasons, the initialisation method makes use of two known facts: firstly, the myofibres capture more than half of the total area of the image and are rather homogeneously coloured; secondly, the colour of the myofibres is approximately determined by the preparation with hematoxylin and eosin. Therefore, all pixels with a colour that is either closer to the histogram mode than a fixed threshold or closer to the a-priori known preparation colour than a fixed threshold are initially assigned to the region of myofibres. All remaining pixels are assigned to the region of connective tissue. After this assignment, the embedding function is smoothed by a Gaussian kernel with standard deviation 2.5 in order to remove small enclosures in both regions. After this procedure, the initial contour, shown in Figure 2b, is in general already a good

approximation of the final contour and less than 200 iterations are sufficient for the active contour to converge.

Refining the segmentation result. Although the active contour model yields accurate boundaries in large parts of the image, some myofibres may not be completely separated from each other (Figure 3a, arrows). Myofibres represent individual skeletal muscle cells. Therefore, the single fibre is well-defined to the surrounding connective tissue by a cell membrane, which causes the strong edges between the homogeneously textured myofibres and the fascicular arranged collagenous fibres of the connective tissue. Therefore, in order to refine the result, a Sobel operator is applied to the original image as edge detector (Figure 3b) and serves as morphological filter which enhances the fibre outlines. The Sobel convolution kernel performs a 2-D spatial gradient measurement on an image and so emphasises regions of high spatial gradient that correspond to edges. The edge detector image is merged with the result of the active contour model in Figure 3a by extracting the average pixel values of all colour channels in both images, resulting in a 8-bit grey value image (Figure 3c). Each muscle fibre region is binarised by applying a threshold to the grey values of pixels forming the region (Figure 3d). For thresholding, we used the mixture modelling method, which automatically selects the proper threshold. This method separates the histogram of an image into two classes using a Gaussian model and then calculates the image threshold as the intersection of these two Gaussians. The resulting binary image is then processed by operations of mathematical morphology (22): irregularities ("holes") within the segmented fibres are eliminated by outlining and refilling the outlined structures, whereas irregularities in the fibre contour are removed by applying the "opening" filter (erosion followed by dilation). The result of this morphological postprocessing is shown in Figure 3e.
The data flow diagram in Figure 5 gives an overview of the main steps of the proposed system.

Morphometric analysis. Different morphometrical parameters for each region of interest (segmented muscle fibres), i.e., fibre cross-sectional area, perimeter, circularity, Feret diameter, and lesser diameter, are calculated automatically by built-in routines of ImageJ (Public Domain, http://rsb.info.nih.gov/ij/). Muscle fibres which are only partially engaged within the picture frame (edged particles) are excluded automatically from analysis. All analysed fibres/structures are outlined, numbered and displayed in the output image (Figure 2d, 3f).

System Performance

A total of 30 digital images containing 679 fibres on five human muscle specimens were segmented by the automated method. The image data was derived from 1) two biopsy samples with no pathological alterations, one of those with very narrow distances between fibres or even partially touching fibres and with low grey value gradient between myofibre and interfibrillar connective tissue (Fig. 4a), 2) two samples with neurogenic atrophy, containing hypertrophic fibres and also nuclear clumps (Fig. 4c), 3) one dystrophic muscle sample with numerous strongly hypotrophic fibres and proliferation of connective tissue (Fig. 2, 3, and 4e), and segmentation results were evaluated independently by two neuropathologists (Y.K. and W.F.), respectively. Each single object, which was regarded by the automated system as a single region of interest and which was concordantly assigned to a single myofibre by the experts were recorded as correctly detected - whereas each region of interest, which did not correspond to a single myofibre, i.e., clustered myofibres, blood vessels, or connective tissue areas, was recorded as falsely segmented. The percentage of correctly detected fibres as displayed in the output images (Fig. 2d) from the total amount of fibres (n=679) was defined as correct classification rate. The inherent parameters of the methodology were kept fixed for all images to ensure a fully automated processing.
Additionally, the accuracy of the morphometric analysis was assessed by comparison between human and machine measurements of 10 out of the 30 digital images containing a total of 191 fibres on five human muscle specimens (normal, neurogenic atrophic, and dystrophic muscle samples as

described above). Three experts traced fibre outlines with a computer mouse using the "freehand" ROI selection tool. Calculation of cross sectional area, perimeter, circularity, and Feret diameter were done automatically by the computer for each outlined fibre. The manually collected data were compared to the machine measurement of the same images and the segmented regions whether obtained by human or machine were compared directly with each other by calculating the percentage of overlapping pixels (overlap ratio). For each fibre, the three human measurements and the results obtained by the automated system were averaged. This was used as standard of comparison. The mean error was defined as the mean of deviations from the standard of comparison assessed for each fibre (Table).

RESULTS

Main steps of the segmentation process are illustrated in Figure 2 and 3. The example image taken from a dystrophic biopsy sample demonstrates the accurate distinction of myofibres from non-myogenic structures by the active contour model (Fig. 2c). In most cases, fibre boundaries are bordered accurately. However, particularly in moderately prepared specimens and highly dystrophic samples, some closely adherent fibres are not completely separated by the active contour. In the final refinement step of the segmentation procedure almost all of these small bridging areas between the fibres are eliminated by the application of the edge-detected image as morphological mask (Fig. 3b).

Direct comparison of the presented approach (Fig. 6b and 6d) with segmentation results obtained by alternative initialisation (Fig. 6a and 6c) or active contour algorithm according to Chan and Vese (Fig. 6e) are displayed exemplarily in Fig. 6. Obviously, the method is not very sensitive to different initialisations. Although the initialisation in Fig. 6a leads to the false segmentation of some blood vessels at the boundary, most of the fibres are segmented correctly. On the other hand, the statistical model and the texture features involved are crucial to deal with such muscle fibre images, as the result obtained with the Chan-Vese method in Fig. 6e reveals.

Additionally, a sensitivity analysis of the segmentation procedure was performed by adding noise to the original images (signal to noise ratio: 5.44). This still yielded accurate segmentation results (Fig. 6f), though the noise reduces the discriminative power of the texture features. Therefore, higher noise levels would decrease the ability of the method to separate single fibres.

The correct classification rate among a total of 679 fibres was high (663 fibres correctly detected: 98%). Neither the mean overlap ratios nor the morphometric data obtained manually or by the computerised automated method did reveal any significant differences. Mean deviations of the morphometric parameters in each of the 191 fibres did not show any significant differences, neither (Table).

Table. Mean overlap ratios, average morphometrical values, and mean error [%] from standard of comparison as assessed for 191 fibres, obtained manually by three investigators and by machine.

	Human 1	Human 2	Human 3	machine
overlap ratio	94.5 %	95.4 %	95.5 %	94.3 %
fibre area	5707 μm^2	5639 μm^2	5617 μm^2	5625 μm^2
	7.6 %	7 %	6.7 %	7 %
perimeter	292.5 µm	301.1µm	301.1µm	302.7µm
	5.6 %	4.1 %	4.3 %	4 %
circularity	0.74	0.70	0.69	0.68
	6.1 %	9.7 %	9.4 %	10.5 %
diameter	111.3 µm	111.4 µm	110.9 µm	111 µm
	3.7 %	4.1 %	3.5 %	3.6 %

DISCUSSION

Despite a great demand for computerised automated procedures in muscle fibre morphometry, there are only few papers dedicated to this topic so far. To date, there are some segmentation approaches based on pixel-intensity and gradient information (4,6,7). In contrast to these semi-automatic segmentation methods, our results suggest that the combined edge and region based active contour approach is suitable for fully automated fibre segmentation and analysis. The accurate segmentation procedure and analysis performance of our automated method deplete the user interaction up to the level of visual supervision. The rate of correctly segmented fibres in our method is even better than in some semi-automatic methods and the performance of measurements is as accurate as manual analysis by experts. A previous prototype of an active contour based method as introduced by Klemenčič (8) also showed acceptable analysis performance, however, the practicability of this prototype was still limited by the necessity of extensive user interaction. First, in order to construct the Voronoi polygons, centroids had to be pointed manually for each fibre. This manual selection of centroids comprises subjectivity and presumes precognition as well as experiences in neuromuscular diagnostics. In our method, the initialisation of the contour detection process is determined fully automatically by a histogram analysis and a thresholding procedure. This is possible, since region based active contours are less sensitive to bad initialisations than their purely edge based predecessors and still yield reasonable results in cases where the initialisation obtained with the thresholding is far from the sought solution. Consequently, a manual definition of fibre centroids is no longer necessary.

Second, Voronoi regions that are unbounded had to be outlined manually. Instead we proposed a refinement of the active contour result by an edge-enhanced mask, which finally leads to a high rate of correctly bounded fibres. Only few fibres in moderately prepared biopsy samples with no visible striplines to adjacent fibres or very thin intermyofibrillar septum with low gradients were falsely segmented and comprised merely 2% of all investigated fibres. Even in highly dystrophic muscle samples with great variations in fibre size and distribution, as well as hypertrophy of connective tissue, fatty degeneration, and amounts of terminally atrophic fibres, nuclear clumps, and regenerative alterations, the morphometric analyses were quite accurate and in direct comparison, the overlap ratios between manual and automatic segmentation results were high.

In muscle fibre image segmentation, the fundamental challenge to overcome is the separation of myofibres from non-fibre structures of same pixel-intensity or colour. Intensity and gradient based methods do not consider further intrinsic myofibre-specific information, and therefore, structures like, i.e., blood vessels, nuclear clumps, resorptive processes, and inflammatory infiltrates cannot be differed from muscle fibres. Since connective tissue may exhibit similar staining intensity and colour, all conventional segmentation methods are restricted to staining for alkaline myosin adenosine-triphosphatase (ATPase) after preincubation at different pH, because the connective tissue is omitted by the ATPase reaction. However, other structures, in particular blood vessels, are also ATPase reactive, and therefore, segmentation results are still inaccurate. This leads to inappropriate segmentation and inaccurate measurement results, particularly in biopsy samples with pathological alterations. In order to cope with this challenge, the presented method exploits three sources of information to separate the classes: firstly, the myofibres can mostly be separated from the remaining tissue by means of the colour, as provided by the sample preparation; secondly, the edge based term from classical active contours exploits the fact that muscle fibres are often separated by more or less strong edges from the connective tissue; thirdly, the texture model respects that the fibre regions are almost homogeneous in contrast to the remaining tissue and thereby adds an additional source of information to the process that has not been taken into account by previous approaches. A further important feature of the proposed method is the implicit representation of the separating contour by a level set function that allows for topological changes. Consequently, the problem of separating a multitude of myofibre regions reduces to the much simpler task of separating the image into two classes, one that captures the area of the myofibres

and one that captures the non-fibre structures. This classification approach enables a reliable and more practicable segmentation of myofibres - even in routinely HE-stained specimens.
In conclusion, the method will prove to be very valuable in high-content image analysis of muscle samples for research purposes as well as in clinical diagnostics. Since the method enables full automation, convenient batch processing of the entire biopsy sample may be possible, and therefore, selection bias could be avoided. The method is easy to use and it neither requests special knowledge in image processing nor special histochemical stains.

References

1. Swash M and Schwartz MS: Neuromuscular diseases. Berlin: Springer; 1988.
2. Mastaglia FL: Skeletal muscle pathology. London: Churchill Livingstone; 1992.
3. Dubowitz V: Muscle biopsy: a practical approach. London: Bailliere Tindall; 1985.
4. Castleman KR, Chui LA, Martin TP, Edgerton VR: Quantitative muscle biopsy analysis. Monogr Clin Cytol. 9:101-116, 1984.
5. Eilbert JL, Gallistel CR, McEachron DL: The variation in user drawn outlines on digital images: Effects on quantitative autoradiography. Comput Med Imaging Graph 14:331-339, 1990.
6. Dudley AW, Spittal RM, Dayoff RE, Ledley RS. Computed image analysis techniques of skeletal muscle. In: Jasmin G, Proschek L, editors. Microanalysis and quantification. Basel: Karger; 1984. p 34-57.
7. Collumbien R, Zukowski F, Claeys A, Roels F: Automated analysis of muscle fibre images. Anal Cell Pathol. 2:373-387, 1990.
8. Klemenčič A, Kovačič S, Pernus F: Automated segmentation of muscle fiber images using active contour models. Cytometry. 32:317-326, 1998.
9. Kass M, Witkin A, Terzopoulos D: Snakes: Active contour models, Int. J. Comp. Vision. 1:321-331, 1988.
10. Dervieux A, Thomasset F: A finite element method for the simulation of Rayleigh-Taylor instability. In: Rautman R, editor. Approximation Methods for Navier-Stokes Problems. Berlin: Springer; 1979. p 145-158.
11. Osher S, Sethian JA: Fronts propagating with curvature-dependent speed: Algorithms based on Hamilton-Jacobi formulations, J Comp Physics 79:12-49, 1988.
12. Caselles V, Kimmel R, Sapiro G: Geodesic active contours, Int J Comp Vision 22:61-79, 1997.
13. Kichenassamy S, Kumar A, Olver P, Tannenbaum A, Yezzi A: Conformal curvature flows: from phase transitions to active vision, Arch Rational Mech Analysis 134:275-301, 1996
14. Chan T, Vese L: Active contours without edges, IEEE Trans Image Proc. 10(2):266-277, 2001
15. Paragios N, Deriche R: Geodesic active regions: A new paradigm to deal with frame partition problems in computer vision, J Vis Comm Image Repr. 13(1/2):249-268, 2002.
16. Brox T, Weickert J: A TV flow based local scale measure for texture discrimination. In: Pajdla T, Matas J, editors. Computer Vision - Proc. 8th Europ Conf on Comp Vision. Berlin: Springer 2004. LNCS 3022:578-590
17. Gabor D: Theory of communication, J. Institut. Electr. Eng. 93: 429-457, 1946.
18.. Bovik AC, Clark M, Geisler WS, Multichannel texture analysis using localized spatial filters, IEEE Trans. Pattern Anal. Mach. Intell. 12(1): 55-73, 1990.
19. Parzen E: On the estimation of a probability density function and the mode. Annals of Math. Statistics, 33:1065-1076, 1962.
20. Rousson M, Brox T, Deriche D: Active unsupervised texture segmentation on a diffusion based feature space. In: Proc 2003 IEEE Conference on Comp Vision and Pattern Recognition, p 699-704.
21. Brox T, Rousson M, Deriche R, Weickert J: Unsupervised segmentation incorporating colour, texture, and motion. In: Petkov N, Westenberg MA, editors. Computer Analysis of Images and Patterns. Berlin: Springer 2003. LNCS 2756:353-360.
22. Soille P: Morphological Image Analysis. Berlin: Springer; 1999.

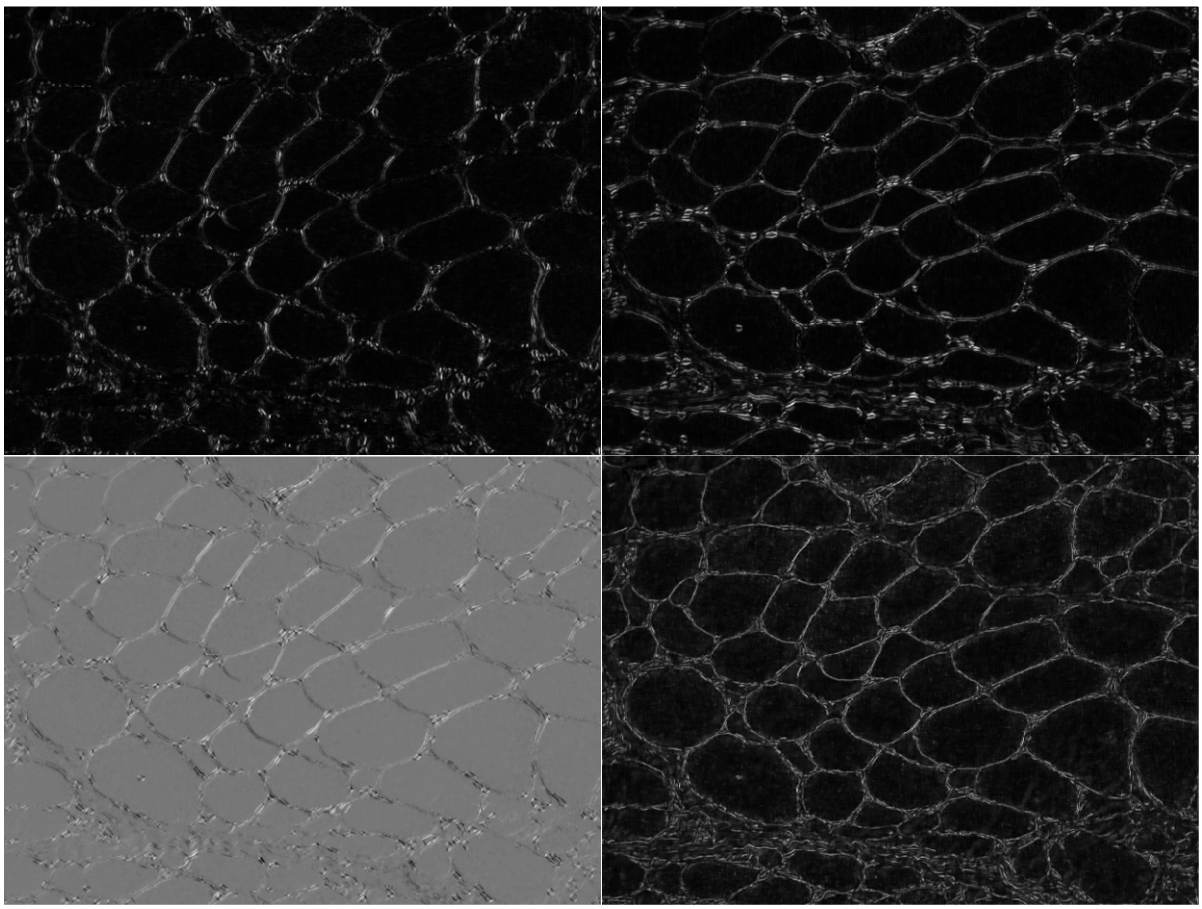

FIG. 1. Texture channels from (16) used in the active contour model. **Top and Bottom Left: (a,b,c)** Components of the structure tensor estimating magnitude and orientation of the texture. **Bottom Right:** (**d)** Local scale measure estimating the scale of texture elements.

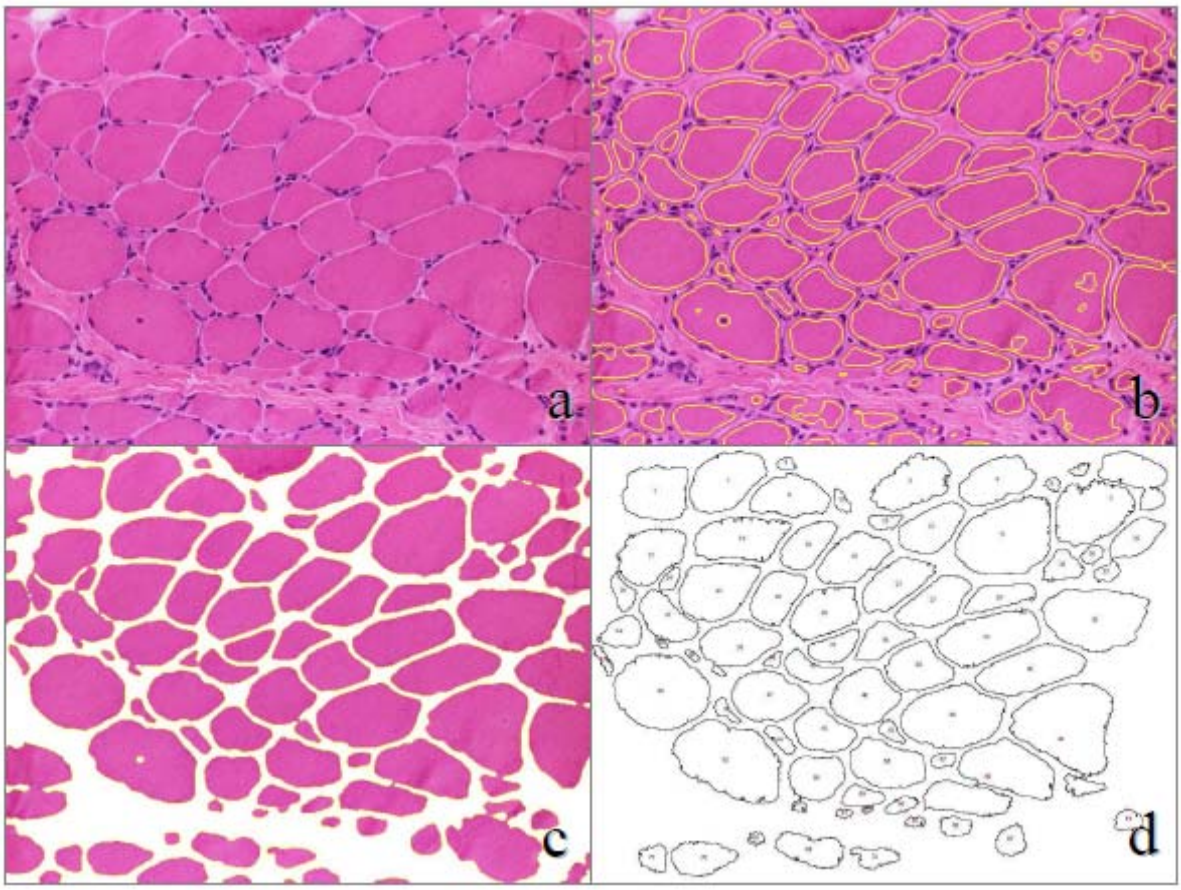

FIG. 2. **a:** Original input RGB image of a dystrophic muscle biopsy sample (cryostat section, HE, x20 objective). **b:** Initial contour depicted in yellow. **c:** Output image of the region based active contour model. The fibre contours are outlined and non-fibre structures are removed. Only myofibres are considered for further morphological processing. **d:** Output image of analysis. Each analysed fibre is outlined and numbered, fibres touching the image boundaries are not considered by the analysis routine.

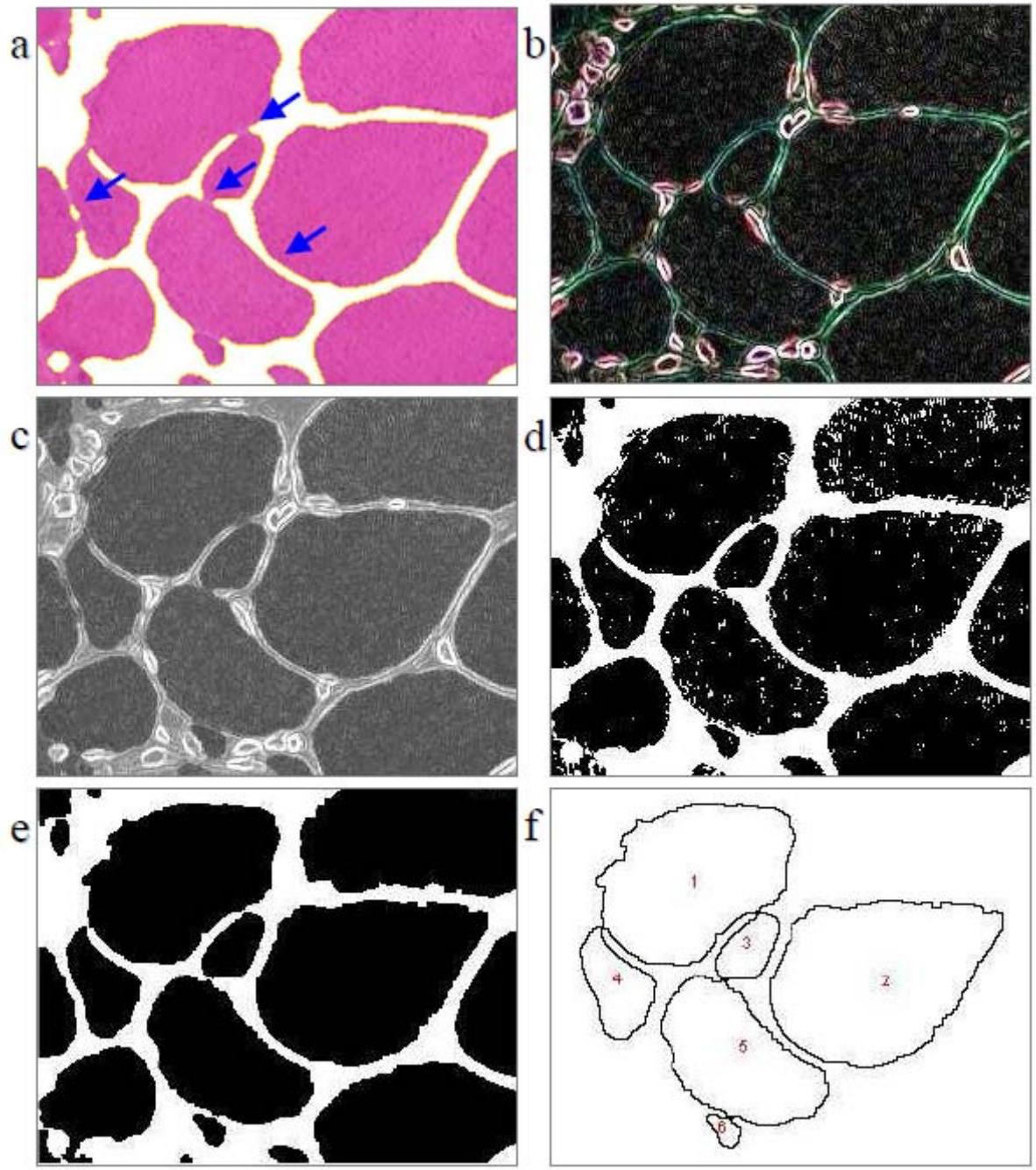

FIG. 3. Steps of refinement for separating adjacent fibres. **a:** Detail from the active contour segmented image of a dystrophic muscle biopsy sample. Fibre boundaries are incompletely bordered in small areas where thin interfibrillar septa are still bridging adjacent fibres (arrows). **b:** Edge-detected image serves as morphological mask with enhanced fibre boundaries. **c:** Active contour segmented image (a) and edge-detector (b) are merged by extraction of average pixel values of both images resulting in a 8-bit image. **d:** Binary image after application of mixture modelling and **e:** morphological operations. Adherenced fibres are completely separated. **f:** Output image after analysis. Each single fibre is correctly segmented and numbered. Edged fibres are excluded automatically from analysis.

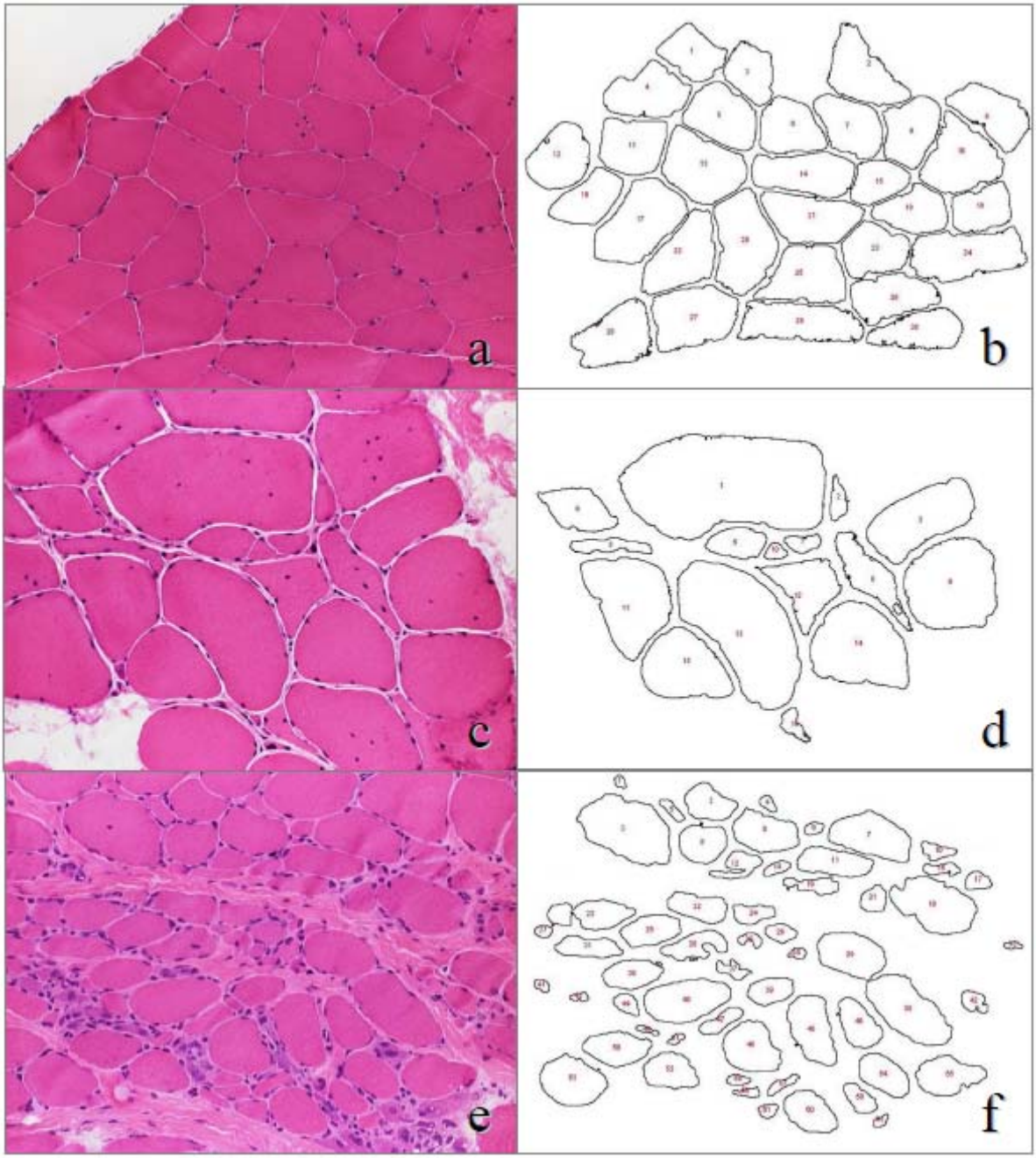

FIG. 4. Morphological variability among the tested image samples, HE, objective x20. **a:** Normal muscle biopsy sample. Intermyofibrillar septa are generally thin, some fibres are attached closely to each other. **c:** Neurogenic alteration with grouped atrophy and compensatory hypertrophy. **e:** Dystrophic muscle biopsy with high level of fibre atrophy and hypertrophy of connective tissue. **b, d**, and **f**: Corresponding output images of automated segmentation and analysis procedures.

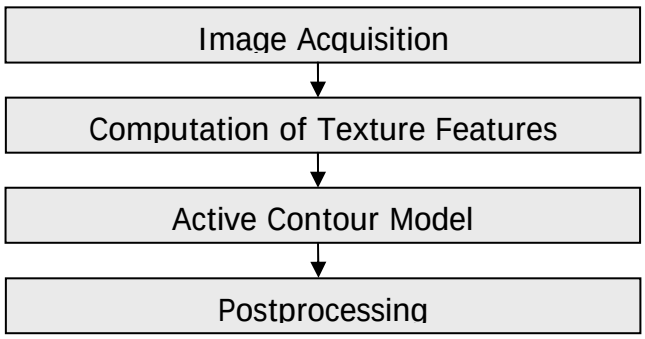

FIG. 5. Data flow diagram highlighting the main steps of the segmentation procedure.

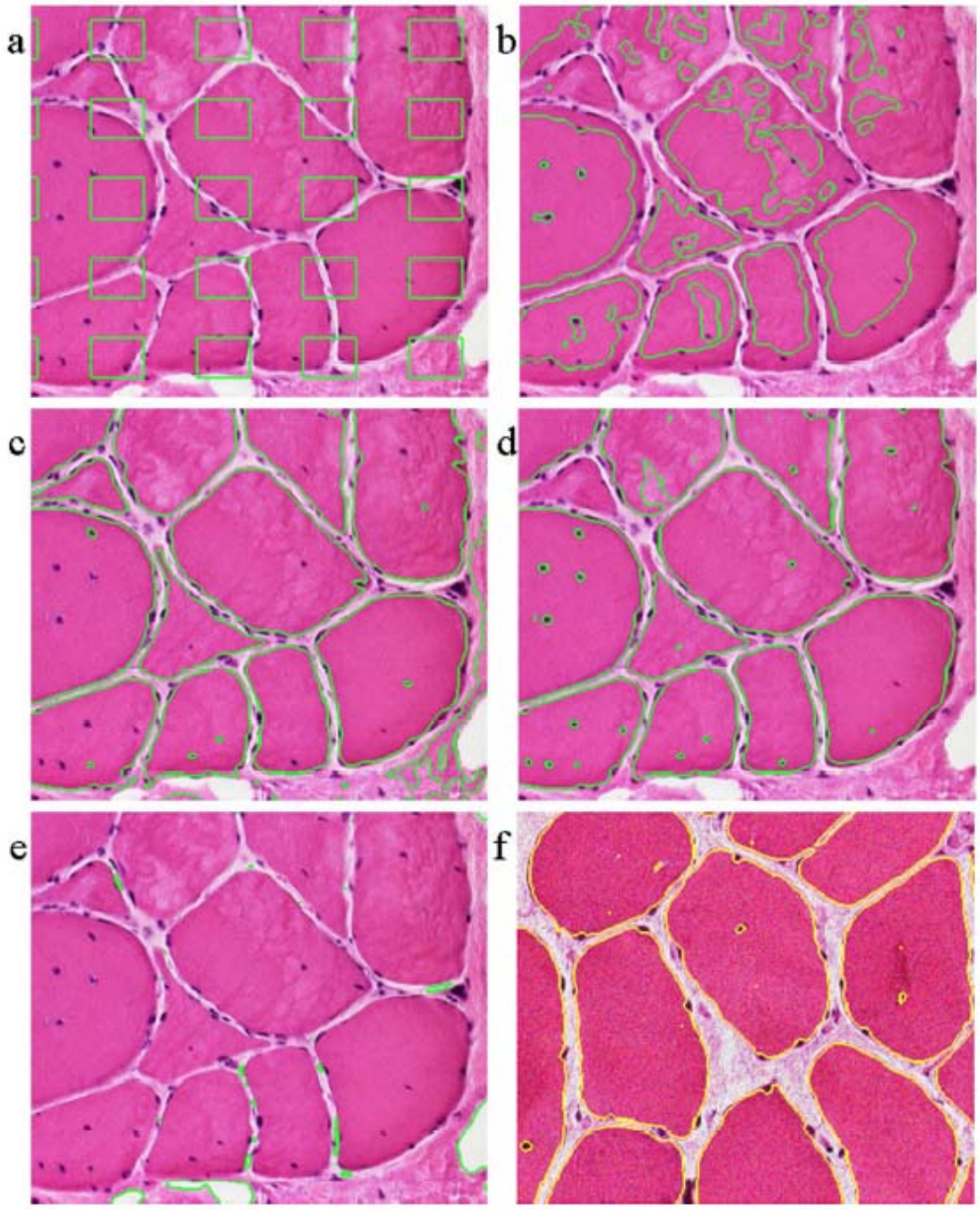

FIG. 6. Comparison of the proposed method with alternative initialisation and segmentation result using the active contour model according to Chan and Vese, HE, objective x20. **a:** Alternative initialisation, **c:** proposed initialisation, and **b, d**: corresponding segmentation results. **e:** Segmentaion result using the active contour model according to Chan and Vese applied to colour images. **f**: Segmentation result of the proposed model after adding noise to the original image (signal to noise ratio: 5.44).